Fish and Shellfish Immunology 93 (2019) 313–321

Contents lists available at ScienceDirect

Fish and Shellfish Immunology

journal homepage: www.elsevier.com/locate/fsi

Full length article

Litopenaeus vannamei Src64B restricts white spot syndrome virus replication by modulating apoptosis

Menghao Wei[a,b,1], Yueling Zhang[a,b,1], Jude Juventus Aweya[a,b], Fan Wang[a,b], Shengkang Li[a,b], Jingsheng Lun[a,b], Chunhua Zhu[c], Defu Yao[a,b,*]

[a] Department of Biology and Guangdong Provincial Key Laboratory of Marine Biotechnology, Shantou University, Shantou, 515063, China
[b] STU-UMT Joint Shellfish Research Laboratory, Shantou University, Shantou, 515063, China
[c] College of Fisheries, Guangdong Ocean University, Zhanjiang, 524025, China

ARTICLE INFO

Keywords:
Shrimp
WSSV
Src64B
Apoptosis

ABSTRACT

The Src family kinases (SFK) are involved in signaling transductions that regulate numerous biological activities including host-virus interaction. These features of SFK have been well explored in vertebrates, however, in shrimp, the invertebrate SFK family member Src64B, has not been characterized and therefore its role in shrimp-virus interaction remains unknown. In this study, two *Litopenaeus vannamei* Src64B isoforms (designated LvSrc64B1 and LvSrc64B2) were first cloned and their role in white spot syndrome virus (WSSV) infection was explored. Bioinformatics analysis revealed that LvSrc64B1 and LvSrc64B2 were similar to other Src64B family members, with high homology in primary and tertiary structures, and contained the conserved SFK functional domains, as well as the putative myristylation and phosphorylation sites. Tissue distribution analysis showed that both LvSrc64B isoforms were ubiquitously expressed, albeit distinctively in the tested tissues. In addition, transcript levels of LvSrc64B1 and LvSrc64B2 were significantly induced following WSSV challenge and had similar expression patterns. Furthermore, siRNA-mediated knockdown of LvSrc64B1 and LvSrc64B2 followed by WSSV infection resulted in increased expression of viral genes, enhanced viral DNA replication, and elevation of hemocytes apoptosis. Depletion of LvSrc64B1 and LvSrc64B2 also reduced shrimp survival upon WSSV infection. In conclusion, the current data strongly suggest that Src64B is a host factor that inhibits WSSV replication by modulating apoptosis in shrimp.

1. Introduction

Penaeid shrimp are one of the most extensively cultured crustacean species, but their aquaculture has been plagued with various bacterial and viral diseases in the past three decades [1,2]. White spot syndrome virus (WSSV) is a highly contagious and lethal DNA virus that causes as much as 90–100% cumulative mortality within 3–10 days upon infection of farmed shrimp [3]. Since its first outbreak in 1992, WSSV has spread globally to all major shrimp farming countries, resulting in huge economic losses to the shrimp farming industry [4]. There is currently no vaccine or effective antiviral method to prevent or to treat WSSV infection. Therefore, there is an urgent need to better understand the shrimp antiviral immune response to WSSV and to identify potential targets so as to be able to develop and/or institute effective viral control and prevention measures.

Src family kinases (SFK) is a family of non-receptor tyrosine kinases. There are nine mammalian SFK members including: c-Src, Yes, Fyn, and Fgr constituting the SrcA subfamily, Lck, Hck, Blk, and Lyn forming the SrcB subfamily, and Frk in its own subfamily [5]. In Drosophila, only two SFK members, namely Src42A and Src64B, have been identified that are functionally similar to mammalian Frk and c-Src, respectively [6]. Upon stimulation, SFK is activated by various cell surface receptors and hence plays crucial roles in diverse cellular processes such as cell proliferation, mobility, adhesion and survival [7,8]. Recently, a growing number of studies have shown that SFK is involved in the regulation of host-virus interaction. For instance, SFK is reported to be required for cell entry by many viruses such as group B coxsackieviruses (CVBs), infectious bursal disease virus (IBDV) and *Bombyx mori* cytoplasmic polyhedrosis virus (BmCPV) [9–11]. Beside their role in viral entry, SFK has also been shown to be hijacked by viruses to promote viral replication, as well as viral assembly and maturation [12–14]. On the other hand, several studies have shown that SFK mediates innate

* Corresponding author. Department of Biology, School of Science, Shantou University, Shantou, Guangdong, 515063, China.
E-mail address: dfyao@stu.edu.cn (D. Yao).
[1] These authors contributed equally to this work.

https://doi.org/10.1016/j.fsi.2019.07.062
Received 4 June 2019; Received in revised form 21 July 2019; Accepted 24 July 2019
Available online 24 July 2019
1050-4648/

antiviral immunity by interacting with Toll-like receptor 3 (TLR3) and retinoic acid-inducible gene-I (RIG-I) as well as with their adaptor proteins [15–17]. Additionally, we previously found that *L. vannamei* Src42A had an antiviral activity by binding to focal adhesion kinase (FAK) and modulating its kinase activity [18].

Src64B, another member of the SFK family in invertebrate, has not yet been identified and/or characterized in shrimp. In the current study, two isoforms of Src64B homolog from *L. vannamei* (dubbed LvSrc64B1 and LvSrc64B2) were first cloned and their role in WSSV infection was explored. Our results revealed that LvSrc64B1 and LvSrc64B2 responded to WSSV infection and restricted virus replication by modulating apoptosis. These findings provide novel insight into the antiviral role of Src64B homolog in shrimp, which would help to better understand the innate immune response of shrimp against viral infection.

2. Materials and methods

2.1. Experimental animals and tissue sampling

Penaeid shrimps (*L. vannamei*), weighing about 5–8 g each, were bought from Shantou Huaxun Aquatic Product Corporation (Shantou, Guangzhou, China), and cultured in aerated seawater at 25 °C for 2 days before experiments. Hemolymph was withdrawn into 500 μL of pre-cooled anti-coagulant solution (336 mM NaCl, 115 mM glucose, 27 mM sodium citrate, 9 mM EDTA-2Na, pH 7.0), and hemocytes pelleted by centrifugation at 700 × *g* for 10 min at 4 °C. Other tissues including the hepatopancreas, gill, intestine, heart, muscle, and stomach were excised and ground immediately in liquid nitrogen and then used for RNA or DNA extraction. All shrimp experiments were performed in line with the guidelines and approval of the Animal Research and Ethics Committees of Shantou University, Guangdong, China.

2.2. Total RNA extraction and cDNA synthesis

Total RNA from the different tissues (hemocytes, hepatopancreas, gill, intestine, heart, muscle and stomach) were extracted using the RNAFast200 kit (FeiJie, Shanghai, China). The concentration of the extracted total RNA was measured using NanoDrop 2000 spectrophotometer (Thermo Scientific, USA), while the quality of the RNA was verified using 1% agarose gel electrophoresis. Thereafter, the total RNA was used for cDNA synthesis with a commercial kit (TransGen Biotech, Beijing, China). The reaction mixture for the cDNA synthesis included 1 μg of total RNA, 10 μL of 2 × TS reaction mix, 1 μL of gDNA remover, 1 μL of *TransScript* RT/RI enzyme mix, 1 μL of anchored Oligo$(dT)_{18}$ primer, plus RNase-free water to a total volume of 20 μL. The mixture was first incubated for 15 min at 42 °C and then inactivated for 5 s at 85 °C. The cDNA was used immediately or stored at −20 °C for later use.

2.3. cDNA cloning of LvSrc64B

The full-length cDNA sequences encoding Src64B (LvSrc64B1 and LvSrc64B2) were obtained from our in-house unpublished *L. vannamei* transcriptome data. Based on this, gene-specific primers were designed (Table 1) and chemically synthesized for use in polymerase chain reaction (PCR) amplification and cloning of the ORFs of LvSrc64B1 and LvSrc64B2. The PCR reactions were carried out in a total reaction volume of 20 μL: 10 μL of 2 × PrimeSTAR premix (Takara, Japan), 1 μL of cDNA, 1 μL each of the forward and reverse primers, and 7 μL of Milli-Q water. The PCR cycling conditions were as follows: one cycle at 98 °C for 3 min, followed by 35 cycles at 98 °C for 10 s, 60 °C for 10 s, 72 °C for 1 min; and a final extension at 72 °C for 10 min. Next, the PCR products were analyzed by 1.5% agarose gel electrophoresis and then purified using EasyPure PCR Purification Kit (TransGen Biotech, Beijing, China). The purified DNA was then digested with *Bam*H I and *Xho* I (Takara, Japan), and inserted into the pET-28a (+) vector (TransGen Biotech, Beijing, China), before being transformed into *Escherichia coli* BL21 (TransGen Biotech, Beijing, China). Positive clones were screened by colony PCR and the sequence confirmed by DNA sequencing (Beijing Genomics Institute, Beijing, China).

Table 1
Sequences of primers and siRNAs used in this study.

Name	Sequence (5′-3′)[a]
For gene cloning	
LvSrc64B–F	CGC**GGATCC**ATGGGCCAGAATATGTGTTGC
LvSrc64B1-R	CCG**CTCGAG**CTAGAAGGCTGCCGCAGCT
LvSrc64B2-R	CCG**CTCGAG**TTAGTCGTGGATGTCGCGA
For qPCR analysis	
LvSrc64B1-q-F	GCGGGTATCGCATGAGTAAGC
LvSrc64B1-q-R	GCAGCTGGCTCATATGTTCGC
LvSrc64B2-q-F	ACCGAGAGGTCATAGAGAAAGTCC
LvSrc64B2-q-R	GATGTCGCGATAGGGTATTTCG
IE1-q-F	GCACAACAACAGACCCTACCC
IE1-q-R	GAAATACGACATAGCACCTCCAC
VP28-q-F	AAACCTCCGCATTCCTGTGA
VP28-q-R	TCCGCATCTTCTTCCTTCAT
LvEF-1α-q-F	TATGCTCCTTTTGGACGTTTTGC
LvEF-1α-q-R	CCTTTTCTGCGGCCTTGGTAG
For RNAi analysis	
siLvSrc64B–F	GGUAUGGUAUGUGGAACAATT
siLvSrc64B-R	UUGUUCCACAUACCAUACCTT
siNon-F	UUCUCCGAACGUGUCACGUTT
siNon-R	ACGUGACACGUUCGGAGAATT

[a] Restriction sites for gene cloning were underlined and highlighted in bold.

2.4. Bioinformatics analysis

Analysis of sequence homology of LvSrc64B1 and LvSrc64B2 was carried out with Basic Local Alignment Search Tool (BLAST) (https://blast.ncbi.nlm.nih.gov/Blast/). Functional and conserved domains were predicted using Simple Modular Architecture Research Tool (SMART) (http://smart.embl.de/), while multiple sequence alignment was performed using DNAMAN software (version 6.0.3.99). Homology modeling of LvSrc64B1 and LvSrc64B2 were performed using SWISS-MODEL program (https://swissmodel.expasy.org/) and further analyzed using PyMOL software (version 1.3.x). A Neighbor-Joining phylogenetic tree was constructed using MEGA5.1 software based on the full-length protein sequences with 1000 bootstrap replicates.

2.5. Tissue distribution

The distribution of LvSrc64B1 and LvSrc64B2 in different shrimp tissues was analyzed using real-time quantitative PCR (qPCR) with gene-specific primers (Table 1). Seven tissues including hemocytes, hepatopancreas, gill, intestine, heart, muscle, and stomach were collected from healthy shrimp and used for total RNA extraction and cDNA synthesis as described in subsections 2.1 and 2.2. The qPCR analysis was performed on a LightCycler 480 (Roche, Switzerland) using SYBR Green PCR master mix (GenStar, Beijing, China). The qPCR reaction mixture contained 10 μL of 2 × RealStar Green power mixture, 1 μL each of forward and reverse primers, 1 μL of cDNA and 7 μL of Milli-Q water. The cycling conditions of the qPCR were as follows: one cycle at 95 °C for 10 min and 40 cycles of 95 °C for 15 s and 60 °C for 30 s. All samples were analyzed in triplicate, with the LvEF1α gene used as the internal control gene, and relative mRNA expression calculated using the $2^{-\Delta\Delta CT}$ method.

2.6. Expression profiles of LvSrc64B post WSSV challenge

The WSSV used for the studies was purified from infected crayfish *Procambarus clarkii* using differential centrifugation before being quantified by spectrophotometry as previously described [19,20]. For

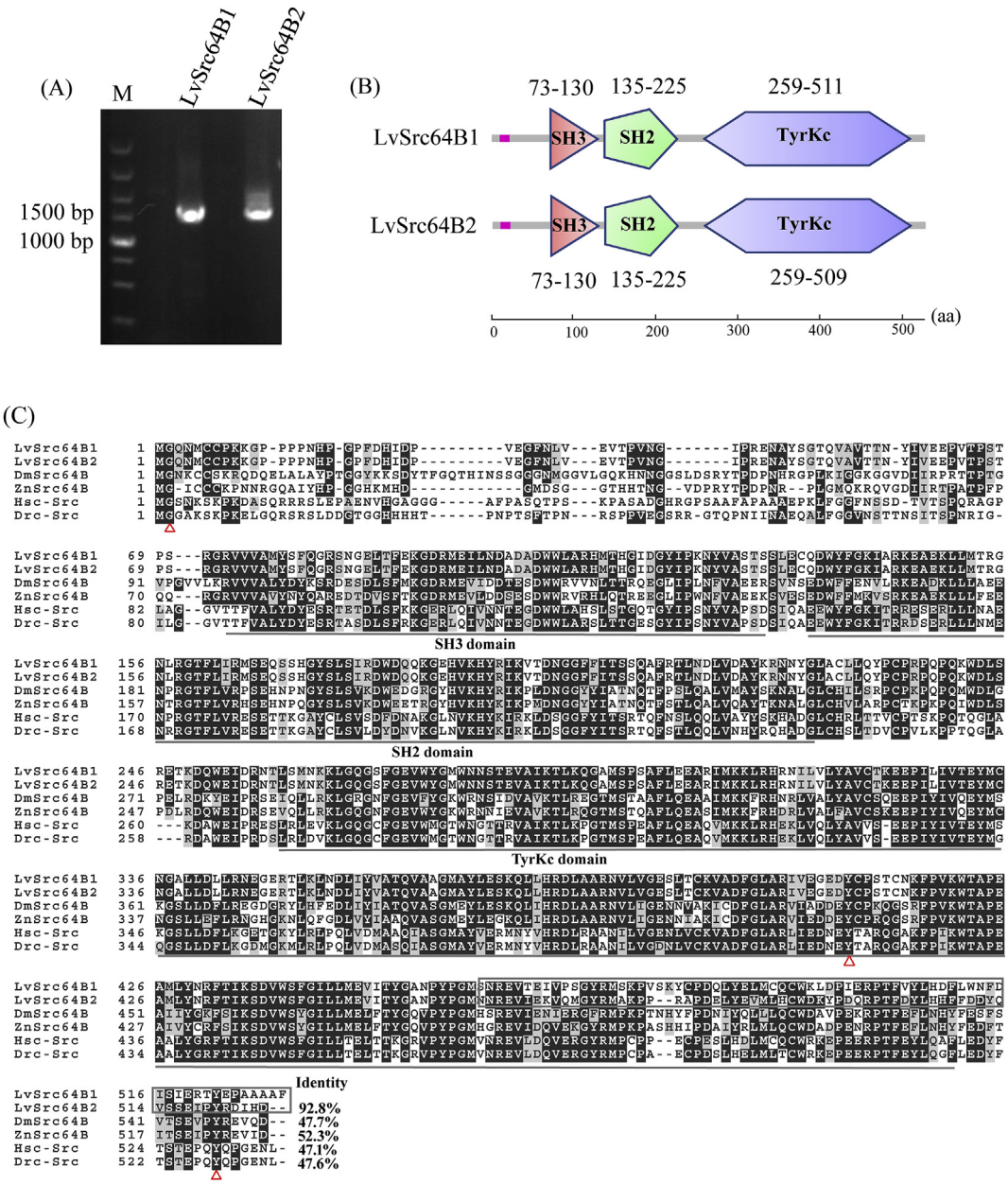

Fig. 1. Cloning and sequence analysis of LvSrc64B. (A) Cloning of the full-length cDNA of LvSrc64B1 and LvSrc64B2 by PCR amplification. M, DNA marker. (B) The predicted functional domains of LvSrc64B1 and LvSrc64B2. (C) Multiple sequence alignment between LvSrc64B and other SFK proteins. The identical amino acid residues are shaded in black and similar residues in gray. The sequence identity between LvSrc64B and other SFK proteins was shown at the end. The conserved domains including SH3, SH2 and TyrKc were underlined, and the myristylation site (Glycine 2) and phosphorylation sites (Tyrosine 409 and Tyrosine 520/522) were indicated by red triangle. The divergent sequence between LvSrc64B1 and LvSrc64B2 was boxed. Proteins used for this analysis include: LvSrc64B1 (*L. vannamei* Src64B1, MH397363), LvSrc64B2 (*L. vannamei* Src64B2, MH397364), DmSrc64B (*Drosophila melanogaster* Src64B, NP_524934), ZnSrc64B (*Zootermopsis nevadensis* Src64B, XP_021923575), Hsc-Src (*Homo sapiens* c-Src, AAH11566) and Drc-Src (*Danio rerio* c-Src, NP_001003837).

WSSV challenge experiments, 100 μL WSSV virions (diluted in PBS, 1×10^6 copies) was intramuscularly injected into shrimp at the third abdominal segment using a 1 mL sterile syringe. Control group shrimp were injected with an equivalent volume of PBS. At 0, 12, 24, 48 and 72 h (h) post challenge, hemolymph from four shrimps per group was collected and pooled before being used for RNA extraction and cDNA synthesis as described in subsection 2.2 above. The mRNA expression of LvSrc64B1 and LvSrc64B2 post infection was then determined by qPCR analysis as described in subsection 2.5. Triplicate experiments were carried out and the results presented as mean ± SD, while statistical analyses were done using the Student's t-test.

2.7. RNA interference assay

To explore the function of LvSrc64B during WSSV infection, the technique of RNA interference (RNAi) was used with specific siRNA designed to target both LvSrc64B1 and LvSrc64B2 (siLvSrc64B) as well as control scrambled siRNA (siNon). The siRNAs were chemically synthesized by Gene-Pharma company (Suzhou, China) and dissolved in DEPC-H_2O prior to use. For the RNAi, shrimps were divided into two groups (20 shrimps per group): one group was intramuscularly injected with 100 μL of 3 μg siLvSrc64B, while the other group was injected with an equal amount of siNon. At 24 h post injection, shrimps from each group were injected again with the same amount of siLvSrc64B or siNon. At 36 h post the first injection, hemocytes were collected from

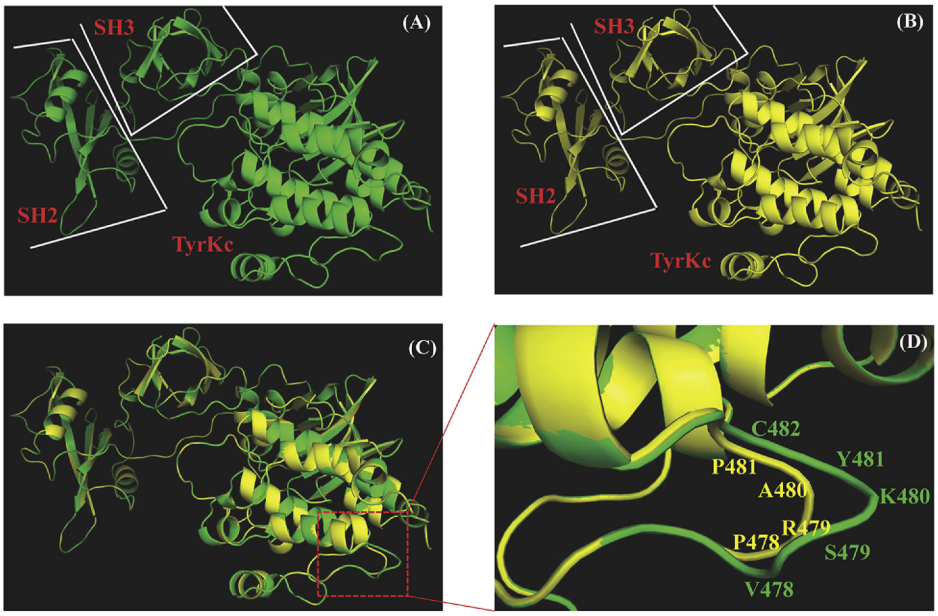

Fig. 2. Tertiary structures of LvSrc64B. Predicted tertiary structure of LvSrc64B1 (A) and LvSrc64B2 (B) based on the template 1y57.1A (sequence identity, 54.24% and 53.57%, respectively) using SWISS-MODEL. The structures of LvSrc64B1 and LvSrc64B2 were merged and compared using PyMOL software (C), and the region that differed was excised and shown as an enlarged image (D).

four shrimps per group for total RNA extraction and determination of knockdown efficiency using qPCR analysis. The remaining shrimps in each group were then challenged with WSSV at 1×10^6 copies per shrimp. At 24 and 48 h post infection, hemocytes from four shrimps per group were pooled and divided into two: one part was used for RNA extraction followed by analysis of WSSV genes expression, while the other part was used to detect caspase3/7 activity. Gills were also collected at the same timepoints (24 h and 48 h) for DNA extraction and determination of WSSV copies. The protocols used to determine viral gene expression, WSSV copies and caspase3/7 activity are described in subsections 2.8 and 2.9.

2.8. Analysis of WSSV genes expression and viral copies

The mRNA expression levels of IE1 (WSSV immediate-early gene) and VP28 (WSSV late gene) in hemocytes were analyzed by qPCR using the primer pairs IE1-q-F/R and VP28-q-F/R, respectively (Table 1).

The WSSV copy number in gills was determined by absolute quantification using a previously described method [21]. Briefly, the ORF of the VP28 gene was obtained by PCR amplification and ligated into the pMD19-T vector (Takara, Japan) by TA cloning. The recombinant plasmid was quantified using a Nanodrop2000 spectrophotometer (Thermo Scientific, USA), and the copy number calculated based on its molecular weight. Next, the plasmid was serially diluted 10-fold (from 10^9 to 10^2 copy/μL) and used to prepare standard samples for qPCR analysis. At the same time, genomic DNA (gDNA) was extracted from gills using a DNA extraction kit (TianGen, Beijing, China) following the manufacturer's instruction. After quantification, the extracted gDNA samples and the serially diluted standard samples, were subjected to qPCR analysis using the primers VP28-qPCR-F/R (Table 1) as described in subsection 2.5. The cycle threshold (Ct) values and copy number of the standard samples were used to plot a standard curve for viral copy quantification. The WSSV copies in the gDNA samples was calculated using the corresponding Ct values from the standard curve. All experiments were carried out in triplicate and the data shown as mean ± SD. Significant differences were analyzed statistically by the Student's t-test.

2.9. Detection of caspase3/7 activity

The caspase 3/7 activity in hemocytes after LvSrc64B knockdown was detected using a Caspase-Glo® 3/7 assay kit (Promega, USA) according to the supplier's manual. Briefly, hemocytes were collected into anti-coagulant buffer and further diluted to a total volume of 10 mL. Next, hemocytes were counted with a hemocytometer (SMOIF, Shanghai, China), and 6 $\times10^3$ cells/well seeded into black 96-well plates. An equal volume of Caspase-Glo® 3/7 assay reagent was added to cells in each well and then incubated for 2 h at room temperature. The reaction mixtures were then transferred into 1.5 mL tubes and subjected to caspase3/7 activity analysis using a GloMax®-Multi Detection System (Promega, USA). Experiments were repeated at least three times and data presented as mean ± SD, while statistical significance were analyzed using the Student's t-test.

2.10. Determination of survival rate

The rate of survival was determined using a survival curve as follows. Shrimps were randomly divided into three groups (15 shrimps/group) and cultured in aerated seawater at 25 °C prior to experiments. Each group was injected twice with 100 μL of siLvSrc64B, siNon or DEPC-H_2O as described above. After 36 h, the siLvSrc64B and siNon-injected groups were then challenged with 100 μL of 1×10^6 WSSV virions, while the DEPC-H_2O-injected group was injected with an equal amount of PBS as the negative control. The number of dead shrimps in each group was recorded at 12 h interval post infection. The survival curve was plotted, and the significant difference was statistically analyzed by log-rank test using GraphPad Prism software (version 7.00).

3. Results

3.1. Cloning, sequence, homology modeling and phylogenetic analysis of LvSrc64B

The full-length cDNA sequences of shrimp Src64B, which were retrieved from our unpublished *L. vannamei* transcriptome data, was used for PCR cloning of the ORFs of LvSrc64B1 and LvSrc64B2 using gene-specific primers (Fig. 1 A). The cloned sequences were confirmed by DNA sequencing and BLAST analysis, before being submitted to the NCBI database under accession numbers MH397363 and MH397364 for LvSrc64B1 and LvSrc64B2, respectively.

The ORF of LvSrc64B1 is 1590 bp in length encoding a putative protein of 529 amino acids (aa), while LvSrc64B2 has an ORF of 1578 bp, encoding a putative protein of 527 aa (Supplementary Fig. S1). Domain prediction analysis showed that both LvSrc64B1 and

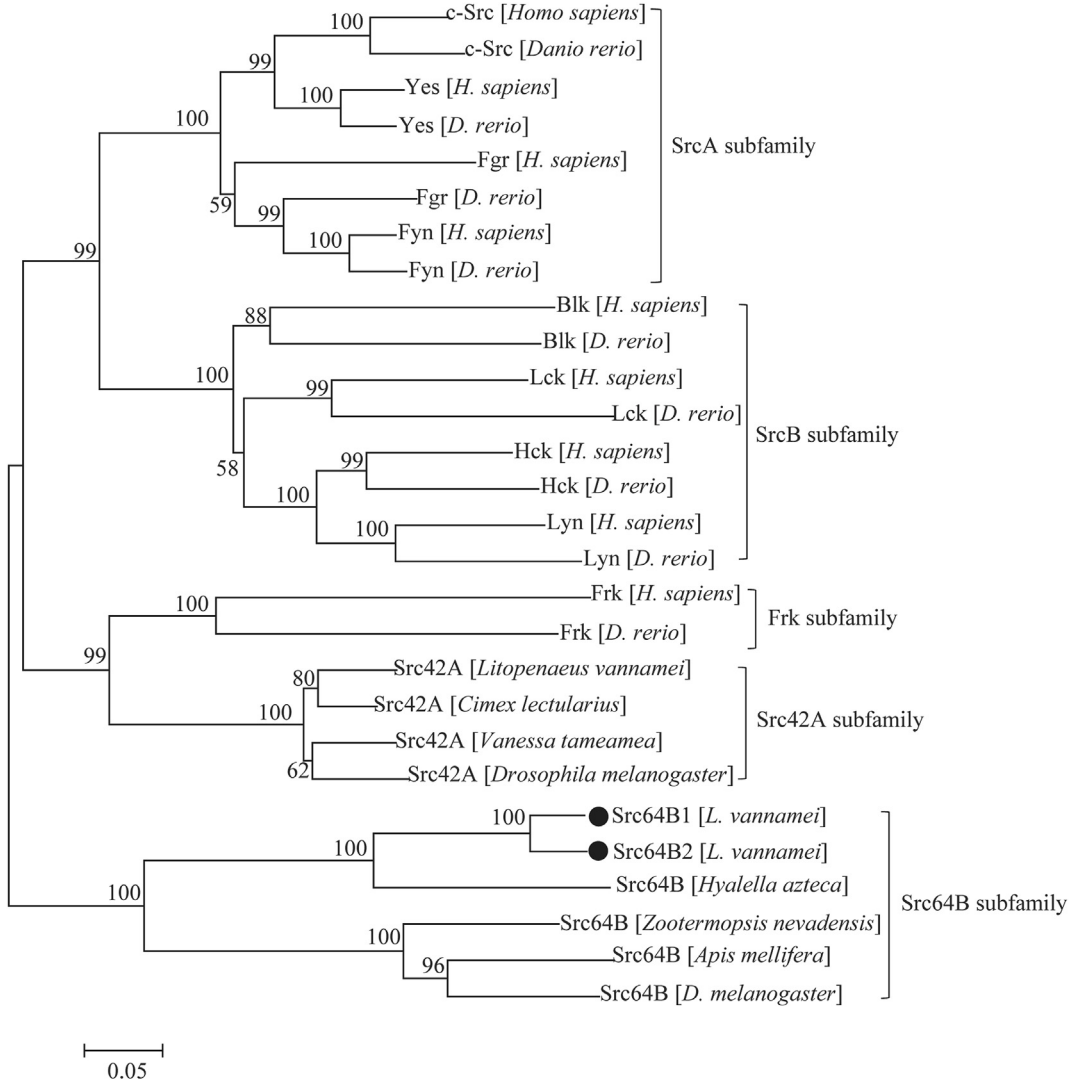

Fig. 3. Phylogenetic tree analysis of LvSrc64B. The numbers marked on the branches indicated the bootstrap values. SFK proteins used in this study were listed below: *Homo sapiens* c-Src (AAH11566), *Danio rerio* c-Src (NP_001003837), *H. sapiens* Yes (NP_005424), *D. rerio* Yes (NP_001013288), *H. sapiens* Fgr (NP_001036194), *D. rerio* Fgr (NP_001352482), *H. sapiens* Fyn (NP_002028), *D. rerio* Fyn (AAX47959), *H. sapiens* Blk (NP_001706), *D. rerio* Blk (NP_001025391), *H. sapiens* Lck (AAH13200), *D. rerio* Lck (NP_001001596), *H. sapiens* Hck (AAI13855), *D. rerio* Hck (XP_005174178), *H. sapiens* Lyn (NP_002341), *D. rerio* Lyn (NP_001004543), *H. sapiens* Frk (NP_002022), *D. rerio* Frk (XP_695937), *L. vannamei* Src42A (ASQ43185), *Cimex lectularius* Src42A(XP_014256379), *Vanessa tameamea* Src42A (XP_026494014), *Drosophila melanogaster* Src42A (NP_476849), *L. vannamei* Src64B1 (MH397363), *L. vannamei* Src64B2 (MH397364), *Hyalella azteca* Src64B (XP_018014858), *Z. nevadensis* Src64B (XP_021923575), *Apis mellifera* Src64B (XP_396908) and *D. melanogaster* Src64B (NP_524934). The location of LvSrc64B1 and LvSrc64B2 is indicated by a black filled cycle.

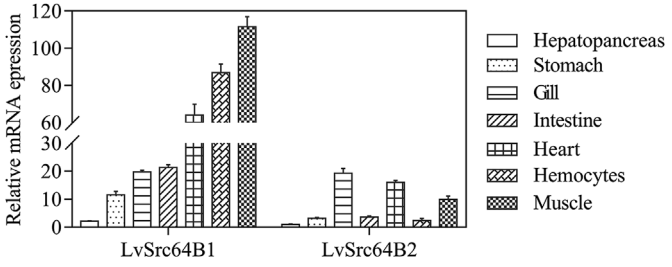

Fig. 4. Tissue distribution of LvSrc64B. The transcript level of LvSrc64B1 and LvSrc64B2 in different tissues was determined using qPCR analysis. LvEF1α was used for internal control gene, and the expression level of LvSrc64B2 in hepatopancreas was set to 1.0.

LvSrc64B2 possess typical SFK functional domains including Src homologous 3 (SH3) domain (73–130 aa), Src homologous 2 (SH2) domain (135–225 aa), and Tyrosine kinase catalytic (TyrKc) domain (259–511 aa in LvSrc64B1 and 259–509 aa in LvSrc64B2) (Fig. 1 B). Multiple sequence alignment analysis revealed that LvSrc64B1 and LvSrc64B2 had 92.8% identity, with sequence diversity only found at the C-terminus (Fig. 1C), indicating that they could be two isoforms of Src64B homolog in shrimp. In addition, LvSrc64B1 and LvSrc64B2 shared more than 40% identity with other SFK family proteins such as *Drosophila melanogaster* Src64B (DmSrc64B) and *Homo sapiens* c-Src (Hsc-Src). Most importantly, LvSrc64B1 and LvSrc64B2 also contain the conserved myristylation site (Glycine 2) and phosphorylation sites (Tyrosine 409 and 522 of LvSrc64B1 and Tyrosine 409 and 520 of LvSrc64B2) (Fig. 1C).

To further determine the functional conservatism of LvSrc64B1 and LvSrc64B2, the tertiary structural models of these two isoforms was predicted using SWISS-MODEL. As shown in Fig. 2A and B, LvSrc64B1 and LvSrc64B2 had very similar tertiary structures, both containing the SH2, SH3 and TyrKc domains. Interestingly, the sequence variance at the C-terminus could not alter the overall tertiary structures of LvSrc64B1 and LvSrc64B2, although some difference could be seen in

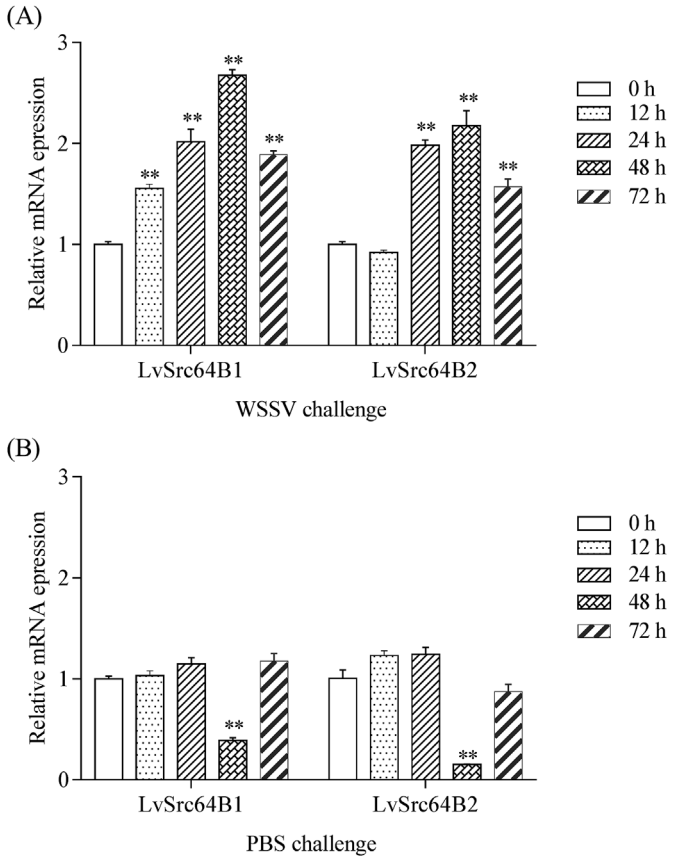

Fig. 5. LvSrc64B was upregulated post WSSV challenge. Expression profiles of LvSrc64B1 and LvSrc64B2 in hemocytes post WSSV (A) or PBS (B) injection at indicated timepoints were determined by qPCR analysis. The mRNA expression levels of LvSrc64B1 and LvSrc64B2 were normalized to those of LvEF-1α using $2^{-\Delta\Delta CT}$ method, and the expression level of LvSrc64B1 and LvSrc64B2 at 0 h post injection was set to 1.0. Results were expressed as mean ± SD of triplicate assays and analyzed statistically by Student's t-test. *, $p < 0.05$, and **, $p < 0.01$.

the random coils (478–481 aa in LvSrc64B1 and LvSrc64B2) within the TyrKc domain (Fig. 2C and D). Furthermore, phylogenetic tree analysis of SFK proteins from various species revealed that they were distinctly grouped into five subfamilies including SrcA, SrcB and Frk for vertebrates, and Src42A and Src64B for invertebrates. LvSrc64B1 and LvSrc64B2 were evolutionarily closer with each other, and clustered with invertebrates Src64B subfamily members (Fig. 3).

3.2. Tissue distribution of LvSrc64B

The transcript levels of LvSrc64B1 and LvSrc64B2 in different shrimp tissues determined by qPCR analysis (Fig. 4), revealed that both were expressed in all tissues tested, albeit with distinct profiles. LvSrc64B1 was highly expressed in muscle, hemocytes and heart, moderately in intestine, gill and stomach, and least in the hepatopancreas. On the other hand, LvSrc64B2 was highly expressed in gill, heart and muscle, moderate in intestine, stomach and hemocytes, and low in the hepatopancreas. Notably, the mRNA expression of LvSrc64B1 was generally higher than that of LvSrc64B2 in all tissues tested.

3.3. LvSrc64B is up-regulated upon WSSV challenge

The response of LvSrc64B to WSSV infection was determined in terms of changes in the mRNA expression of LvSrc64B1 and LvSrc64B2 in hemocytes at different timepoints post challenge. As shown in Fig. 5 A, the transcript levels of LvSrc64B1 and LvSrc64B2 followed a similar expression pattern post WSSV infection, with both being up-regulated from 0 h to 48 h and then down-regulated at 72 h. The peak expression for both LvSrc64B1 and LvSrc64B2 was at 48 h post infection, which was about 2.67-fold and 2.17-fold, respectively, compared to baseline expression level at 0 h. The expression of LvSrc64B1 and LvSrc64B2 did not change in the PBS control group throughout the experimental time points (Fig. 5 B). These results suggest that LvSrc64B1 and LvSrc64B2 are involved in WSSV infection, probably synergistically.

3.4. LvSrc64B inhibits WSSV replication in vivo

To further explore the role of LvSrc64B in WSSV infection, the technique of RNAi was employed. Two groups of shrimps were injected twice (0 h and 24 h) with gene-specific siRNA (siLvSrc64B) or scramble control siRNA (siNon). At 36 h post the first injection, hemocytes were collected and the knockdown efficiency of LvSrc64B1 and LvSrc64B2 was evaluated by qPCR analysis. The qPCR result in Fig. 6 A revealed significant ($p < 0.05$) decrease in the expression of LvSrc64B1 and LvSrc64B2 compared with control, which indicates successful *in vivo* knockdown of LvSrc64B1 and LvSrc64B2. Next, the siLvSrc64B or siNon-injected shrimps were then challenged with WSSV, and the expression levels of WSSV genes (IE1 and VP28) as well as the WSSV copy number were determined. The mRNA expression levels of WSSV IE1 (Fig. 6 B) and VP28 (Fig. 6C) as well as the viral copy number (Fig. 6 D) in siLvSrc64B-injected shrimp at 24 and 48 h post WSSV infection were significantly ($p < 0.05$ and $p < 0.01$) higher compared with the siNon-injected control group (Fig. 6 B, C and D) at the same time points post WSSV infection. These data suggest that LvSrc64B plays an antiviral role by inhibiting WSSV replication *in vivo*.

3.5. LvSrc64B plays anti-apoptotic and defensive role during WSSV infection

To determine the potential antiviral mechanism of LvSrc64B, we went on to investigate the effect of LvSrc64B knockdown on host immune response during WSSV infection. Given that SFK plays a critical role in cell survival [22], we first examined whether LvSrc64B depletion could affect hemocytes apoptosis during WSSV infection. It was observed that knockdown of LvSrc64B followed by WSSV infection resulted in significant ($p < 0.05$ and $p < 0.01$) increase in hemocytes caspase 3/7 activity at 24 and 48 h post WSSV infection compared with control (Fig. 7 A). This suggest an increase in hemocytes apoptosis upon LvSrc64B depletion in shrimp. Next, shrimp survival was analyzed after LvSrc64B depletion followed by WSSV infection. As shown in (Fig. 7 B), the survival rate of shrimp depleted of LvSrc64B (LvSrc64B1 and LvSrc64B2) and infected with WSSV was significantly ($p < 0.05$) reduced compared with the siNon control. For instance, it was observed that the survival rate of LvSrc64B-depleted shrimps decreased sharply and reached zero at 36 h post infection, while the survival rate of shrimps in the siNon control group was more than 23% at the same time point. On the other hand, the negative control shrimp maintained a very high survival rate (~70%) throughout the experimental period. The results thus indicated that LvSrc64B knockdown could result in attenuation in the ability of shrimp to resist WSSV infection, which suggest that LvSrc64B might play an anti-apoptotic and/or defensive role during WSSV infection.

4. Discussion

The Src family kinase (SFK) is involved in signaling transductions that control various biological processes including cell proliferation, mobility, adhesion and survival [23]. Some SFK members have been implicated in regulating host-virus interaction through the modulation of viral entry and replication, which signify their importance in viral infection and antiviral immune response [9,13,14,16]. Moreover, our previous studies revealed that *L. vannamei* Src42A was involved in

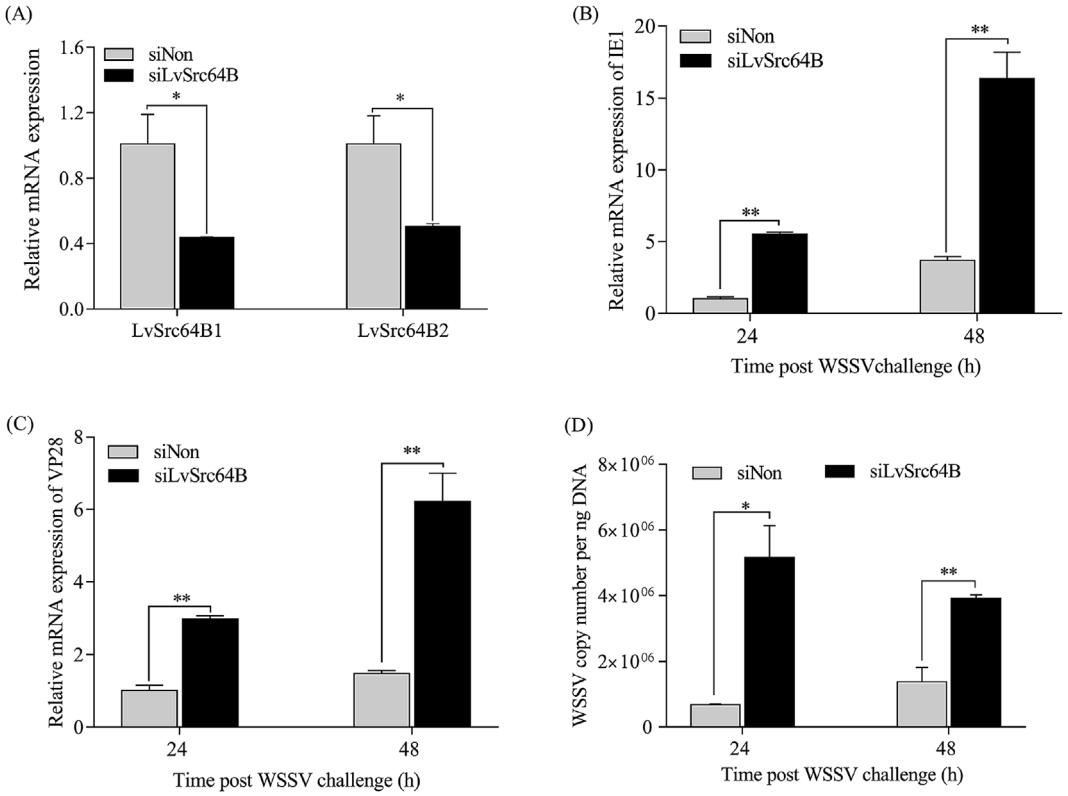

Fig. 6. LvSrc64B knockdown promoted WSSV replication *in vivo*. Shrimps were injected twice (0 and 24 h) with siLvSrc64B and siNon, respectively. At 36 h post the first injection, hemocytes of each group were harvested and used for determination of the RNAi efficiency by qPCR (A). After confirming the knockdown effect, the rest of shrimps were further challenged with WSSV. At 24 h and 48 h post infection, hemocytes from each group were collected and used for expression analysis of the viral IE1 gene (B) and VP28 gene (C) by qPCR analysis. Meanwhile, the gill tissues of each group were collected and subjected to quantification of WSSV copy number (D) by qPCR analysis. All the qPCR analyses were performed in triplicate for each sample, and the data were shown as mean ± SD and analyzed statistically by Student's t-test. *, $p < 0.05$, and **, $p < 0.01$.

immune defense against WSSV infection by regulating the FAK signaling cascade [18]. At present, only two SFK family members have been identified in invertebrates, i.e., Src42A and Src64B in fruit fly [24] and Src42A in shrimp [18]. However, shrimp Src64B has not yet been reported and little is therefore known about its role in WSSV infection. This prompted us to explore shrimp Src64B homologs and examined their possible role in WSSV infection.

Here, we cloned and characterized two previously unreported Src64B isoforms (LvSrc64B1 and LvSrc64B2) from shrimp *L. vannamei*. Bioinformatics analysis revealed that both LvSrc64B1 and LvSrc64B2 were highly similar in primary and tertiary structures, with both containing the conserved SH3, SH2 and TyrKc domains (Figs. 1 B and Fig. 2) of SFK [25]. In addition, LvSrc64B1 and LvSrc64B2 also possessed the putative myristylation and phosphorylation sites (Fig. 1C). It has been well established in mammals that myristylation is required for targeting SFK to membranes, while phosphorylation is involved in SFK activation [22]. Given that LvSrc64B1 and LvSrc64B2 contain these conserved features suggest they have similar regulatory mechanisms i.e., through myristylation and phosphorylation, and therefore might play similar physiological and pathological functions in shrimp. Tissue distribution analysis revealed that LvSrc64B1 and LvSrc64B2 were ubiquitously expressed in shrimp tissues (Fig. 4), which is consistent with the wide distribution of SFK members in different species [18,26,27]. Notably, the transcript levels of LvSrc64B1 was much higher in tissues such as muscle, hemocytes and heart than LvSrc64B2 in the same tissues (Fig. 4). In mammals, the alternative spliced isoforms of c-Src and Fyn have also been reported to be highly expressed in some specific cell types and tissues compared to others [23].

As key mediators in host-virus interaction [28], SFK have also been reported by a growing studies to promote viral infections [29–31] and mediate antiviral immune responses in various organisms [32,33]. In this study, the mRNA expression levels of LvSrc64B1 and LvSrc64B2 were significantly elevated upon WSSV challenge, which suggest the involvement of LvSrc64B in WSSV infection (Fig. 5 A). This observation is synonymous to the expression of *L. vannamei* Src42A in response to WSSV infection [18]. Given that the expression of both isoforms of LvSrc64B (LvSrc64B1 and LvSrc64B2) followed a similar pattern upon WSSV infection, suggest that they function synergistically during viral infection. The role of LvSrc64B in WSSV infection was then explored using the technique of RNAi. Knockdown of LvSrc64B1 and LvSrc64B2 significantly increased transcript levels of WSSV early (IE1) and late (VP28) genes, as well as enhanced the number of viral copies (Fig. 6 B - D), which suggest that LvSrc64B is a host factor that inhibits WSSV replication *in vivo*.

Since invertebrates' Src64B performs similar functions as c-Src in vertebrates [6], couple with the fact that c-Src is reported to be pro-survival and therefore plays an essential role in the control of cell survival [34–36], we wondered whether shrimp Src64B was involved in apoptosis regulation during WSSV infection. Intriguingly, knockdown of LvSrc64B1 and LvSrc64B2 followed by WSSV infection resulted in an elevation in hemocytes apoptosis, in terms of significant increase in caspase3/7 activity (Fig. 7 A). Given that apoptosis is also a cellular defense mechanism against viral infection [37,38], we inferred that LvSrc64B might play an antiviral role by inhibiting cell apoptosis in WSSV-infected shrimp so as to constraint the virus and therefore prevent the spread to uninfected cells. Notably, this antiviral response mechanism by LvSrc64B is different from previous studies, where c-Src was shown to associate with various components of TLR3 and RIG-1 signaling pathways to elicit interferon-mediated innate antiviral response [15,16,32]. A key role of LvSrc64B in anti-WSSV response was

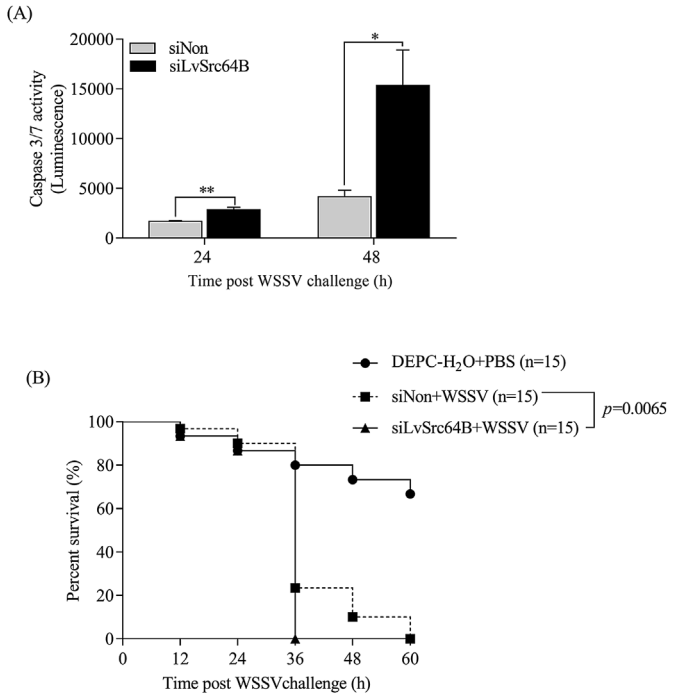

Fig. 7. LvSrc64B knockdown increased cell apoptosis and shrimp death post WSSV infection. (A) Apoptosis analysis of Lv-Src64B-depleted shrimp challenged with WSSV. Shrimps were injected twice (0 and 24 h) with siLvSrc64B and siNon, respectively. After knockdown for 36 h, shrimps of each group were further infected with WSSV. At 24 h and 48 h post infection, hemocytes of each group were collected for detection of caspase 3/7 activity. (B) Survival analysis of LvSrc64B-depleted shrimp infected with WSSV. Shrimp were divided into three groups (15 shrimps per group), and each group was injected twice (0 and 24 h) with siLvSrc64B, siNon or DEPC-H_2O. After 36 h, the siLvSrc64B and siNon-injected groups were further injected with WSSV, while the DEPC-H_2O-injected group was injected with PBS as the negative control. The death number was monitored every 12 h intervals after infection. The survival curve of each group was plotted using the GraphPad Prism 7.0 software, and difference was analyzed with log-rank test, $p = 0.0065$.

further substantiated using shrimp survival analysis. Shrimp depleted of LvSrc64B were more susceptible to WSSV infection, with significant reduction in shrimp survival rate after infection compared with the siNon-injected control (Fig. 7 B). This observation further indicates that LvSrc64B plays anti-apoptotic and defensive role during WSSV infection in shrimp.

In conclusion, this study is the first to report on two homologs of Src64B isoforms (LvSrc64B1 and LvSrc64B2) from shrimp *L. vannamei*. The present results revealed that both LvSrc64B1 and LvSrc64B2 played a synergistic antiviral role in shrimp by modulating apoptosis. These findings would further our understanding of shrimp antiviral immunity, and therefore help in identifying more potential targets for virus control and prevention.

Conflicts of interest

The authors declare that there is no conflict of interest.

Acknowledgments

This work was supported by the National Natural Science Foundation of China (Nos. 31702387 & 31872596), China Postdoctoral Science Foundation (No. 2018M630973), Natural Science Foundation of Guangdong Province (No. 2017A030311032) and Department of Education of Guangdong Province (No. 2017KZDXM033).

Appendix A. Supplementary data

Supplementary data to this article can be found online at https://doi.org/10.1016/j.fsi.2019.07.062.

References

[1] T.W. Flegel, Historic emergence, impact and current status of shrimp pathogens in Asia, J. Invertebr. Pathol. 110 (2) (2012) 166–173.
[2] G.M. Tandel, K.R. John, M. Rosalind George, M.J. Prince Jeyaseelan, Current status of viral diseases in Indian shrimp aquaculture, Acta Virol. 61 (2) (2017) 131–137.
[3] J.H. Leu, F. Yang, X.B. Zhang, X. Xu, G.H. Kou, C.F. Lo, Whispovirus, Curr. Top. Microbiol. Immunol. 328 (2009) 197–227.
[4] J.G. Sánchez-Martínez, G. Aguirre-Guzmán, H. Mejía-Ruíz, White spot syndrome virus in cultured shrimp: a review, Aquacult. Res. 38 (13) (2010) 1339–1354.
[5] A.L. Hughes, Evolution of the src -related protein tyrosine kinases, J. Mol. Evol. 42 (2) (1996) 247–256.
[6] M.J. Williams, The c-src homologue Src64B is sufficient to activate the Drosophila cellular immune response, J. Innate Immun. 1 (4) (2009) 335–339.
[7] S.J. Parsons, J.T. Parsons, Src family kinases, key regulators of signal transduction, Oncogene 23 (48) (2004) 7906–7909.
[8] J. Espada, J. Martín-Pérez, An update on Src family of nonreceptor tyrosine kinases biology, Int. Rev. Cell Mol. Biol. 331 (2017) 83–122.
[9] C.B. Coyne, J.M. Bergelson, Virus-induced Abl and Fyn kinase signals permit coxsackievirus entry through epithelial tight junctions, Cell 124 (1) (2006) 119–131.
[10] C.J. Ye, X.P. Han, Z.L. Yu, E. Zhang, L.J. Wang, H.B. Liu, Infectious bursal disease virus activates c-Src to promote α4β1 integrin-dependent viral entry by modulating the downstream Akt-RhoA GTPase-actin rearrangement cascade, J. Virol. 91 (3) (2016) e01891-16.
[11] Y.L. Zhang, L.Y. Zhu, G.L. Cao, M. Sahib Zar, X.L. Hu, Y.H. Wei, R.Y. Xue, C.L. Gong, Cell entry of BmCPV can be promoted by tyrosine-protein kinase Src64B-like protein, Enzym. Microb. Technol. 121 (2019) 1–7.
[12] J.S. Shin, E. Jung, M. Kim, R.S. Baric, Y.Y. Go, Saracatinib inhibits middle east respiratory syndrome-coronavirus replication *in vitro*, Viruses 10 (6) (2018) E283.
[13] A.J. Hirsch, G.R. Medigeshi, H.L. Meyers, V. DeFilippis, K. Fruh, T. Briese, W.I. Lipkin, J.A. Nelson, The Src family kinase c-Yes is required for maturation of West Nile virus particles, J. Virol. 79 (18) (2005) 11943–11951.
[14] J.J. Chu, P.L. Yang, c-Src protein kinase inhibitors block assembly and maturation of dengue virus, Proc. Natl. Acad. Sci. U.S.A. 104 (9) (2007) 3520–3525.
[15] I.B. Johnsen, T.T. Nguyen, M. Ringdal, A.M. Tryggestad, O. Bakke, E. Lien, T. Espevik, M.W. Anthonsen, Toll-like receptor 3 associates with c-Src tyrosine kinase on endosomes to initiate antiviral signaling, EMBO J. 25 (14) (2006) 3335–3346.
[16] I.B. Johnsen, T.T. Nguyen, B. Bergstroem, K.A. Fitzgerald, M.W. Anthonsen, The tyrosine kinase c-Src enhances RIG-I (retinoic acid-inducible gene I)-elicited antiviral signaling, J. Biol. Chem. 284 (28) (2009) 19122–19131.
[17] Y.J. Lim, J.E. Koo, E.H. Hong, Z.Y. Park, K.M. Lim, O.N. Bae, J.Y. Lee, A Src-family-tyrosine kinase, Lyn, is required for efficient IFN-beta expression in pattern recognition receptor, RIG-I, signal pathway by interacting with IPS-1, Cytokine 72 (1) (2015) 63–70.
[18] D.F. Yao, L.W. Ruan, J.X. Xu, H. Shi, X. Xu, Characterization of a novel non-receptor tyrosine kinase Src from *Litopenaeus vannamei* and its response to white spot syndrome virus infection, Fish Shellfish Immunol. 68 (2017) 377–385.
[19] X.X. Xie, H.Y. Li, L.M. Xu, Y. Feng, A simple and efficient method for purification of intact white spot syndrome virus (WSSV) viral particles, Virus Res. 108 (1–2) (2005) 63–67.
[20] Q. Zhou, Y.P. Qi, F. Yang, Application of spectrophotometry to evaluate the concentration of purified white spot syndrome virus, J. Virol. Methods 146 (1–2) (2007) 288–292.
[21] S.X. Zhan, J.J. Aweya, F. Wang, D.F. Yao, M.Q. Zhong, J.H. Chen, S.K. Li, Y.L. Zhang, *Litopenaeus vannamei* attenuates white spot syndrome virus replication by specific antiviral peptides generated from hemocyanin, Dev. Comp. Immunol. 91 (2019) 50–61.
[22] R. Robert, Src protein-tyrosine kinase structure, mechanism, and small molecule inhibitors, Pharmacol. Res. 94 (2015) 9–25.
[23] S.M. Thomas, J.S. Brugge, Cellular functions regulated by Src family kinases, Annu. Rev. Cell Dev. Biol. 13 (1997) 513–609.
[24] B.G. Fernández, B. Jezowska, F. Janody, Drosophila actin-capping protein limits JNK activation by the Src proto-oncogene, Oncogene 33 (16) (2014) 2027–2039.
[25] J.R. Engen, T.E. Wales, J.M. Hochrein, M.A.M. Iii, S.B. Ozkan, I. Bahar, T.E. Smithgall, Structure and dynamic regulation of Src-family kinases, Cell. Mol. Life Sci. 65 (19) (2008) 3058–3073.
[26] Q. Zhang, X.Y. Song, P. Su, R. Li, C. Liu, M. Gou, H. Wang, X. Liu, Q.W. Li, A novel homolog of protein tyrosine kinase Fyn identified in *Lampetra japonica* with roles in the immune response, Gene 579 (2) (2016) 193–200.
[27] C. Jopling, J. den Hertog, Fyn/Yes and non-canonical Wnt signalling converge on RhoA in vertebrate gastrulation cell movements, EMBO Rep. 6 (5) (2005) 426–431.
[28] M.A. Pagano, E. Tibaldi, G. Palù, A.M. Brunati, Viral proteins and Src family kinases: mechanisms of pathogenicity from a "liaison dangereuse, World J. Virol. 2 (2) (2013) 71–78.
[29] C.Y. Cheng, W.R. Huang, P.I. Chi, H.C. Chiu, H.J. Liu, Cell entry of bovine ephemeral fever virus requires activation of Src-JNK-AP1 and PI3K-Akt-NF-κB pathways as well as Cox-2-mediated PGE2/EP receptor signalling to enhance clathrin-mediated virus endocytosis, Cell Microbiol. 17 (7) (2015) 967–987.

[30] J. Zhang, X. Lei, D. Wang, Y. Jiang, Y. Zhan, M. Li, Y. Zhou, Y. Qin, J. Liu, A. Wang, Y. Yang, N. Wang, Inhibition of Abl or Src tyrosine kinase decreased porcine circovirus type 2 production in PK15 cells, Res. Vet. Sci. 124 (2019) 1–9.
[31] R. Broeckel, S. Sarkar, N.A. May, J. Totonchy, C.N. Kreklywich, P. Smith, L. Graves, V.R. DeFilippis, M.T. Heise, T.E. Morrison, N. Moorman, D.N. Streblow, Src family kinase inhibitors block translation of Alphavirus subgenomic mRNAs, Antimicrob. Agents Chemother. 63 (4) (2019) e02325-18.
[32] X. Li, M. Yang, Z. Yu, S. Tang, L. Wang, X. Cao, T. Chen, The tyrosine kinase Src promotes phosphorylation of the kinase TBK1 to facilitate type I interferon production after viral infection, Sci. Signal. 10 (460) (2017) eaae0435.
[33] M.M. Hu, W.R. He, P. Gao, Q. Yang, K. He, L.B. Cao, S. Li, Y.Q. Feng, H.B. Shu, Virus-induced accumulation of intracellular bile acids activates the TGR5-beta-arrestin-SRC axis to enable innate antiviral immunity, Cell Res. 29 (3) (2019) 193–205.
[34] J. Schlessinger, New roles for Src kinases in control of cell survival and angiogenesis, Cell 100 (3) (2000) 293–296.
[35] L. Xing, A.M. Venegas, A. Chen, L. Garrett-Beal, B.F. Boyce, H.E. Varmus, P.L. Schwartzberg, Genetic evidence for a role for Src family kinases in TNF family receptor signaling and cell survival, Genes Dev. 15 (2) (2001) 241–253.
[36] L.D. Nelin, H.A. White, Y. Jin, J.K. Trittmann, B. Chen, Y. Liu, The Src family tyrosine kinases, src and yes, have differential effects on inflammation-induced apoptosis in human pulmonary microvascular endothelial cells, Am. J. Physiol. Lung Cell Mol. Physiol. 310 (9) (2016) L880–L888.
[37] H. Everett, G. Mcfadden, Apoptosis: an innate immune response to virus infection, Trends Microbiol. 7 (7) (1999) 160–165.
[38] J.H. Leu, S.J. Lin, J.Y. Huang, T.C. Chen, C.F. Lo, A model for apoptotic interaction between white spot syndrome virus and shrimp, Fish Shellfish Immunol. 34 (4) (2013) 1011–1017.